PREPRINTS

5TH INTERNATIONAL WORKSHOP ON WAVE HINDCASTING AND FORECASTING

JANUARY 26-30, 1998

MELBOURNE, FL

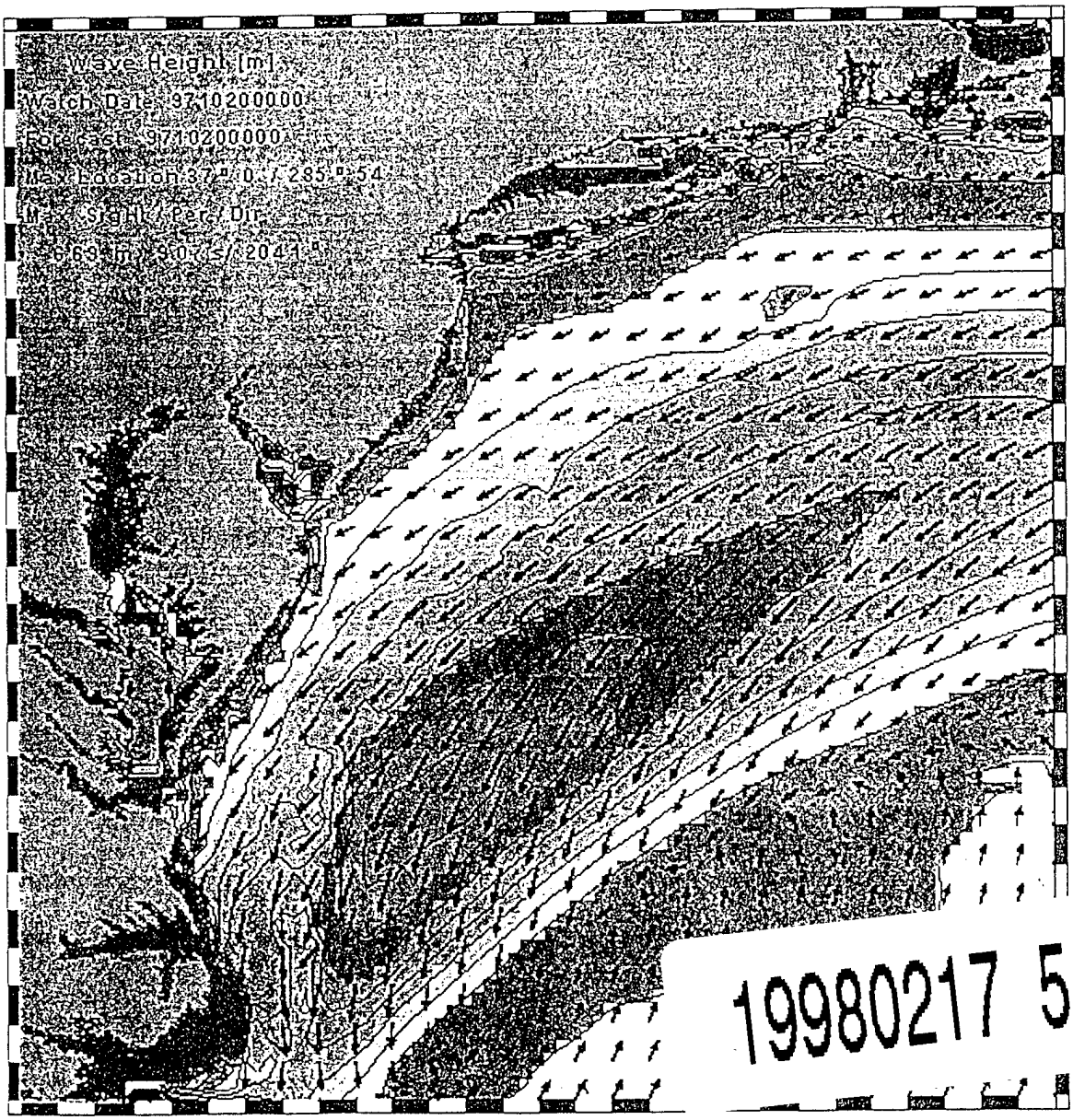

USAE WATERWAYS EXPERIMENT STATION

FLEET NUMERICAL METEOROLOGY AND OCEANOGRAPHY CENTER

FLORIDA INSTITUTE OF TECHNOLOGY

ATOMOPHERIC ENVIRONMENT SERVICE CANADA

REPORT DOCUMENTATION PAGE

Form Approved
OBM No. 0704-0188

1. AGENCY USE ONLY *(Leave blank)*	2. REPORT DATE	3. REPORT TYPE AND DATES COVERED
	January 1998	Proceedings

4. TITLE AND SUBTITLE

Comparison of Model Output of Wind and Wave Parameters with Spaceborne Altimeter Measurements

5. FUNDING NUMBERS

Job Order No. 73680008
Program Element No. 062435N
Project No.
Task No.
Accession No.

6. AUTHOR(S)

Paul A. Hwang, Steven M. Bratos[1], William J. Teague, David W. Wang[2], Gregg A. Jacobs, and Donald T. Resio[1]

7. PERFORMING ORGANIZATION NAME(S) AND ADDRESS(ES)

Naval Research Laboratory
Oceanography Division
Stennis Space Center, MS 39529-5004

8. PERFORMING ORGANIZATION REPORT NUMBER

NRL/PP/7332--97-0025

9. SPONSORING/MONITORING AGENCY NAME(S) AND ADDRESS(ES)

Office of Naval Research
800 North Quincy Street
Arlington, VA 22217-5000

U.S. Army Corps of Engineers
Vicksburg, MS 39180-6199

10. SPONSORING/MONITORING AGENCY REPORT NUMBER

11. SUPPLEMENTARY NOTES

Proceedings of 5th International Workshop on Wave Hindcasting and Forecasting, January 26-30, 1998, Melbourne, FL
[1]U.S. Army Engineer Waterways Experiment Station, Vicksburg, MS 39180-6199
[2]Computer Science Corporation, Stennis Space Center, MS 39529-5004

12a. DISTRIBUTION/AVAILABILITY STATEMENT

Approved for public release; distribution is unlimited.

12b. DISTRIBUTION CODE

13. ABSTRACT *(Maximum 200 words)*

One of the major issues in the hindcasting and forecasting of winds and waves is the difficulty of validation and verification. While comparisons with point measurements from discrete and sparsely distributed wave buoys provide some measure of statistical confidence, the spatial distribution of the modeled wind and wave fields cannot be easily assessed.

Remote sensing from space provides a synoptic view of the ocean wind and wave fields. For example, wind speed and significant wave height are standard output of spaceborne altimeters such as TOPEX/POSEIDON (hereafter referred to as TOPEX for brevity). Comparisons of the altimeter measured wind speed and wave height with surface buoy data have shown very positive agreement. With an along-track resolution of 7 km, the spatial resolution of the spaceborne altimeter is comparable with that of the numerical models used for regional simulations. In the following, we present the results of a comparison study of WAM wave modeling of the Yellow and East China Seas (YES) with two of the TOPEX tracks in the region. In the next section the accuracy of TOPEX altimeter wind and wave measurements is summarized based on earlier studies of TOPEX and surface buoy comparisons. Section 3 describes the YES data sets and the background information about the numerical modeling and satellite tracks in the comparison region. Section 4 presents the results of the comparison in terms of statistics such as bias (B), rms difference (Δ), regression coefficient (c and c_y, to be further discussed later) and correlation coefficient (R). Since altimeter remote sensing provides a spatial coverage of the wind and wave fields along transects, we will explore the use of such information for the validation of wave height distribution from a numerical wave model output. The conclusions and summary are presented in the last section of the paper.

14. SUBJECT TERMS

spaceborne altimetry, ocean modeling, wind parameters, wave parameters, forecasting, hindcasting, remote sensing, TOPEX/POSEIDON, buoys, bathymetry, microwave radars, backscattering, Gulf of Mexico, and WAM

15. NUMBER OF PAGES

10

16. PRICE CODE

17. SECURITY CLASSIFICATION OF REPORT	18. SECURITY CLASSIFICATION OF THIS PAGE	19. SECURITY CLASSIFICATION OF ABSTRACT	20. LIMITATION OF ABSTRACT
Unclassified	Unclassified	Unclassified	SAR

COMPARISON OF MODEL OUTPUT OF WIND AND WAVE PARAMETERS WITH SPACEBORNE ALTIMETER MEASUREMENTS

Paul A. Hwang[1], Steven M. Bratos[2], William J. Teague[1], David W. Wang[3], Gregg A. Jacobs[1] and Donald T. Resio[2]
[1] Oceanography Division, Naval Research Laboratory, Stennis Space Center, MS 39529-5004
[2] U.S. Army Engineer Waterways Experiment Station, Vicksburg, MS 39180-6199
[3] Computer Science Corporate, Stennis Space Center, MS 39529-5004

1. INTRODUCTION

One of the major issues in the hindcasting and forecasting of winds and waves is the difficulty of validation and verification. While comparisons with point measurements from discrete and sparsely distributed wave buoys provide some measure of statistical confidence, the spatial distribution of the modeled wind and wave fields cannot be easily assessed.

Remote sensing from space provides a synoptic view of the ocean wind and wave fields. For example, wind speed and significant wave height are standard output of spaceborne altimeters such as TOPEX/POSEIDON (hereafter referred to as TOPEX for brevity). Comparisons of the altimeter measured wind speed and wave height with surface buoy data have shown very positive agreement (e.g., Ebuchi and Kawamura 1994; Freilich and Challenor 1994; Gower 1996; Hwang et al. 1997). With an along-track resolution of 7 km, the spatial resolution of the spaceborne altimeter is comparable with that of the numerical models used for regional simulations. In the following, we present the results of a comparison study of WAM wave modeling of the Yellow and East China Seas (YES) with two of the TOPEX tracks in the region. In the next section the accuracy of TOPEX altimeter wind and wave measurements is summarized based on earlier studies of TOPEX and surface buoy comparisons. Section 3 describes the YES data sets and the background information about the numerical modeling and satellite tracks in the comparison region. Section 4 presents the results of the comparison in terms of statistics such as bias (B), rms difference (Δ), regression coefficient (c and c_y, to be further discussed later) and correlation coefficient (R). Since altimeter remote sensing provides a spatial coverage of the wind and wave fields along transects, we will explore the use of such information for the validation of wave height distribution from a numerical wave model output. The conclusions and summary are presented in the last section of the paper.

2. ALTIMETER MEASUREMENT OF WIND AND WAVES

Extensive studies of altimeter measurements of wind and wave parameters have been published (e.g., Brown et al. 1981; Chelton and Wentz 1986; Wu 1992; Witter and Chelton 1994; Freilich and Challenor 1994; Ebuchi and Kawamura 1994; Gower 1996; Hwang et al. 1997, and the references therein). These studies have shown consistently that the significant wave height derived from the altimeter is essentially identical to that measured by ocean surface buoys. Particularly, if the distances between the buoy location and the satellite footprints are within 10 km, the rms difference of the two sets of data is approximately 0.14 m. One exception is in the coastal region, where large disagreement often occurs. The cause of the discrepancy may be due to the land effect on radar backscatter or the greater spatial inhomogeneity of the coastal wave field within the radar footprint. There are no established rules relating the deterioration of wind/wave data to the land proximity. Factors effecting the distance of data deterioration include the satellite approach (from land or from sea), the local bathymetry gradient, and the plane geometry of the subject location and shoaling factor. From examining the satellite output, it is estimated that if the satellite approach is from land to sea, three to four footprint lengths (20 to 30 km) are needed for the signal to adjust to the change of backscattering characteristics between land and water. For the sea to land approach, this distance is reduced to one footprint (7 km), but other factors mentioned above may dictate the application distance from land. Since the issue concerning land proximity has not been thoroughly investigated, we will exclude data within 50 km of land in the following comparison.

Derivation of wind speed from microwave radars is based on the correlation of surface roughness and radar backscatter intensity (the normalized radar backscatter cross section, σ_0). For the spaceborne altimeters, specular reflection is the primary mechanism of radar backscatter. In this mode, roughness on the surface causes incident radar waves to diffuse and scatter away from the aperture of radar reception, and the smoother the surface the higher the backscatter is expected. On the ocean surface, short ocean waves are the primary contributor to the surface roughness. Because these short water waves are wind generated, higher σ_0 corresponds to lower wind speed and vise versa. Over the past two decades, the operational algorithms to

retrieve wind speed from the altimeter backscatter cross section, however, have been based on empirical formulae established on collocated databases of altimeter and surface measurements (e.g., Brown et al. 1981; Chelton and Wentz 1986; Witter and Chelton 1991) or on the statistical distributions of wind speeds and σ_0 separately (Freilich and Challenor 1994). These comparisons indicate that despite the continuous improvement of altimeter hardware and software, the progress of wind speed retrieval from various algorithms developed over the last 20 years only shows marginal improvement. For example, Freilich and Challenor (1994) report a very comprehensive analysis of eight algorithms. Results in terms of the mean error (bias), root mean square error, standard deviation, wind speed error trend and pseudo-wave age error trend are tabulated. The differences in all eight algorithms are relatively minor. In terms of mean square errors and standard deviations, 7 of the 8 algorithms produced less than 10% difference in these two error parameters (1.60 to 1.75 m/s rms error, 1.58 to 1.72 m/s standard deviation). When applied to a regional scale, the error statistics are slightly better. For example, comparison of 3.2 years of TOPEX data with 4 buoys in the Gulf of Mexico suggests that when the separation distance between the TOPEX footprint and the buoy location is less than 10 km, the rms difference is approximately 1.2 m/s (Hwang et al. 1997). Figure 1 shows an example of the comparison of significant wave height and wind speed measured by the TOPEX Ku-band altimeter and the surface buoys in the Gulf of Mexico.

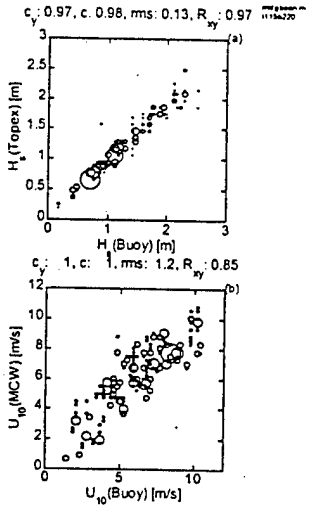

Figure 1. Comparison of the significant wave height and wind speed measured by the TOPEX altimeter and the ocean buoys in the Gulf of Mexico (Hwang et al. 1997).

The regression coefficient, rms difference and correlation coefficient for the wave height are 0.98, 0.13 m and 0.97, respectively; the corresponding statistics for the wind speed are 1.0, 1.2 m/s and 0.85 for this case.

3. YELLOW AND EAST CHINA SEAS DATA SET

As illustrated in the last section, the altimeter output of winds and waves represents a good source of wind/wave measurements for the study of regional wind/wave climate. The data can also be used for verification and validation of wave model output and offer insight into the spatial distribution, which can not be verified easily with point measurements. This is especially valuable in regions where in-situ data are either nonexistent or inaccessible.

The WAM model (Cycle 4) (WAMDI Group 1988; Janssen 1991) was recently applied to the Yellow and East China Seas to hindcast the wave climatology for 1994. The wave hindcast setup consisted of a global 1° Lat/Lon grid to generate input wave boundary conditions and a regional 0.25 ° Lat/Lon grid including the Yellow Sea, East China Sea, and the Sea of Japan shown in Figure 2.

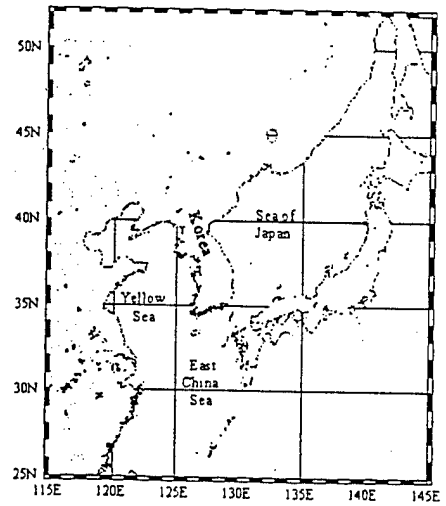

Figure 2. The model domain of the WAM simulation for the year 1994 used in this simulation.

A global wind product (Wobus and Kalnay 1995) from the National Centers for Environmental Prediction (NCEP, formerly the National Meteorological Center) was used to drive the global and regional wave model grids. The NCEP winds, which are provided at approximately 0.94° Lat/Lon resolution, were bilinearly interpolated to a 1° resolution for the global hindcast and a 0.25° resolution for the regional hindcast. The global hindcast was run with a temporal resolution of 6 hours, which is the resolution provided by NCEP. The NCEP

winds were linearly interpolated to a 3 hour resolution for the regional hindcast.

Several researchers have suggested improvements to WAM (Tolman 1992; Lin and Huang 1996; Bender 1996). Bratos (1997) compared deepwater WAM results to National Data Buoy Center (NDBC) wave measurements along the US Atlantic coast using high quality winds (Cardone 1992) for five extratropical storms which included a variety of conditions ranging from extreme events to more moderate and variable events. One persistent tendency found in the WAM results was a low bias significant wave height (SWH), H_S. Figure 3 shows the relationship between wind speed bias and SWH bias for all buoy locations and storm events considered. For a well behaved model the SWH bias should correspond to the wind speed bias. The plot shows a tendency for WAM SWH to be biased low (0.0 m to -0.5 m) when the wind speed is biased high (0.0 m/s to 1.75 m/s).

One of the standard WAM output files includes the SWH, friction velocity $u*$, and drag coefficient C_D at every grid point. The model wind speed at a 10 m elevation is given by $U_{10} = u_* C_D^{-1/2}$. The SWH and wind speed model parameters were extracted along the two TOPEX tracks for comparison. The first track is number 69, a descending track that runs along the central axis of the YES region (Figure 4), and the second track is number 26, which is an ascending track cutting across the entrance region.

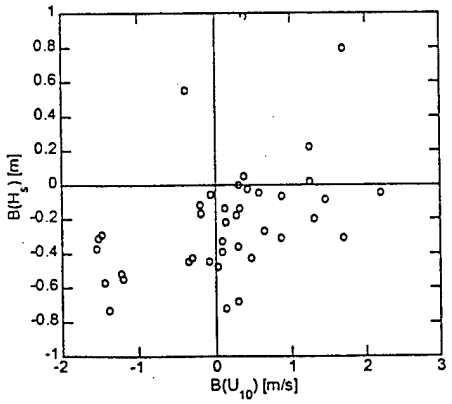

Fig. 3. Example of WAM output compared with buoy measurements along the U. S. Atlantic coast [Bratos 1997].

The extraction of the model output consisted of interpolation of the model parameters to the satellite track coordinates using two subroutines within the GMT-System (General Mapping Tools) (Wessel and Smith 1991). The subroutine *surface* (Smith and Wessel 1990) creates a binary grid file using an adjustable tension continuous curvature algorithm. The subroutine *grdtrack* samples this 2-D binary grid file along tracklines 26 and 69 using bicubic interpolation. The numerical output and altimeter data are then merged together by linear interpolation using the latitude coordinate to a uniform spacing of 0.05 degree in latitude. The spacing between neighboring data points in the merged data set is between 6.0 to 6.3 km along track. The distances between the model data positions and the interpolated altimeter footprints are between 0.4 to 0.6 km. Over the one-year (1994) model run, 32 cycles are extracted for each track (4 of the missing cycles occur at Julian days 63, 172, 311 and 361 for track 26, and 76, 176, 315 and 324 for track 69.). The time differences between the model output and TOPEX measurement are distributed approximately evenly between 0 to 1.5 hours.

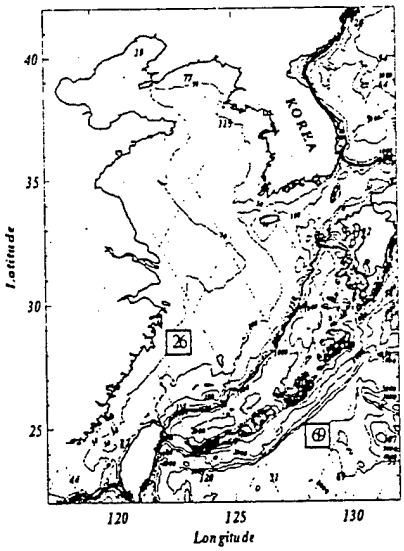

Figure 4. A map of the Yellow and East China Seas (YES) region for this comparison study. TOPEX tracks are shown in dotted curves. Tracks 69 (from NW to SE going through the axis of the region) and 26 (from SW to NE across the YES entrance) are used for comparing with the WAM model simulation for the year 1994.

4. COMPARISON AND DISCUSSIONS

4.1. Average Comparison

We first study the wave and wind climate derived from TOPEX measurements and WAM output. The annual averages along the two tracks are listed in Table 1(A). The statistical distribution of the winds and waves in four different regions designated as are shown in Figure 5 (top half), in which the histogram of wind speeds and wave heights are displayed. These four regions are designated as D9, S3, M3 and N3 for 9 degrees (latitude), Southern 3 degrees, Middle 3

degrees and Northern 3 degrees along the two tracks. The limiting latitudes are tabulated in the first column of Table 1. From these tabulated statistics, it is found that the average properties of wind speed and wave height between the numerical simulation and the remote sensing measurement are in excellent agreement. Both the mean and standard deviation of these average quantities are mostly in agreement within 10 percent. Both TOPEX and WAM show that the average wave height decreases persistently northward. Along the central axis of YES (track 69) the 3-degree average wave height is reduced from 1.70 m at 29°, to 1.49 m at 32° and 1.16 m at 35° based on TOPEX measurements.

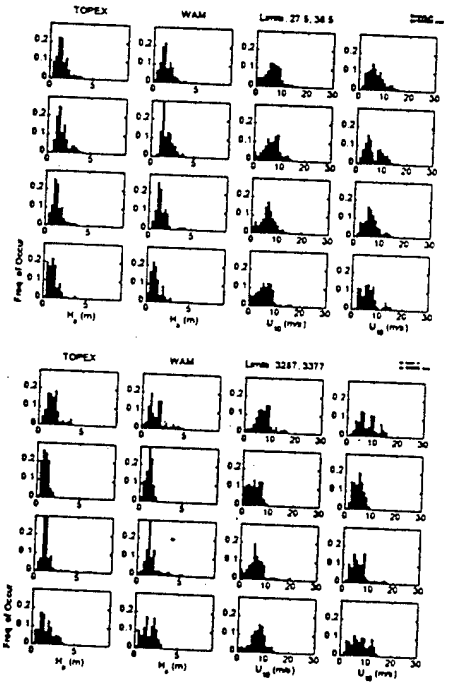

Figure 5. Comparison of the histograms of wave heights and wind speeds from TOPEX measurements and WAM output. The plots are arranged as H_S (TOPEX), H_S (WAM), U_{10} (TOPEX) and U_{10} (WAM) in the first to the fourth column. The upper four rows of the plots are annual data within 9°, Southern 3° (S3), Middle 3° (M3), and Northern 3° (N3), respectively, along track 69. The lower four rows are the histograms of the wind and wave parameters in the 9° latitude along track 69, and over the first to the fourth 90-day period of 1994 data sets.

The results show that the WAM hindcast of the wave heights are slightly higher, by 9%, 3% and 4% respectively, than the TOPEX data for the three regions (S3, M3 and N3). The average wave height along track 26 shows a similar trend, with 1.82 m at 27°, 1.63 m at 30° and 1.51 m at 33°. The WAM output again overpredicts the wave height by 9%, 11% and 2%, respectively. The distribution of the average wave heights can be measured in terms of the standard deviation (Table 1). In the along-axis direction (track 69), the dimensionless standard deviations (normalized by the mean) are 0.45, 0.65 and 0.58 from South to North based on the TOPEX data, and 0.37, 0.55, and 0.74, respectively, based on the WAM output. The standard deviations along track 26 of TOPEX and WAM are in much better agreement ([0.54, 0.47, 0.69] of TOPEX as compared to [0.52, 0.53, 0.61] of WAM). In general, the annual average predicted by WAM model agrees very well with the TOPEX measurement. One of the major sources of discrepancies is the wind speed or wind stress used to drive the model. As shown in Table 1, the average wind speed used in WAM is in general higher than the TOPEX observations. Except for one case (track 69, S3), the WAM average wind is 4 to 19% higher than the corresponding TOPEX data.

The comparison statistics of the seasonal average wave height and wind speed between TOPEX and WAM are also listed in Table 1(B). The histograms of the wave height and wind speed distributions are shown in Figure 5 (lower half). These statistics are based on the data along the full 9-degree tracks discussed above. The statistics over a smaller or larger distance can be generated also. Two of the notable features of the seasonal average are (1) the lower average occurs in the second quarter, and (2) the largest variation as represented by the standard deviation occurs in the third quarter (Table 1B). These features are consistent with the monsoon climate of the region, with predominantly northwesterly to northerly winds in the winter, and southwesterly to southeasterly winds in the summer. In the transition seasons, the winds fluctuate between the two dominant weather systems (e.g., Wang and Aubery 1987). The wind and wave properties are further complicated by the typhoons, which generally occur from July to October, and explain the large variation (standard deviation) of the seasonal statistics during the third quarter. The agreement of the mean properties derived from WAM output and TOPEX measurement is generally good, the ratio of the averages (WAM/TOPEX) ranges between 0.94 to 1.19. The agreement in the standard deviation statistics is also similar to that of the seasonal means. The larger difference in the seasonal means (up to 19% higher, as compared to 11% maximum in the annual means) is closely related to the wind condition used in driving the wave model. The maximum difference of the seasonal average wind speed is 36% (6.5/4.78=1.36; Track 26, Q2) as compared to 19% in the annual means (7.76/6.50=1.19; Track 26, M3).

We then compare the statistical correlation of the WAM and TOPEX along each track. The region of comparison, defined by the latitude distance along the tracks, is varied from less than 1 degree to 9 degrees. The mean properties averaged within the specified region will be presented below. The statistic parameters of the linear regression coefficients c_y and c, the bias, the rms difference and the correlation coefficient are computed and summarized in Table 2. The coefficient c is calculated by minimizing the orthogonal distances between data points to the linear regression curve. In the scatter plot of WAM data vs. TOPEX data with the intercept forced to zero, the regression fitting can be expressed as $y = cx$, where y is the WAM wave height (wind speed) and x is the TOPEX wave height (wind speed). The formula of the orthogonal regression coefficient is described in Bauer et al. (1992) and also in Romeiser (1993),

$$c = \tan\left[\frac{1}{2}\tan^{-1}\left(\frac{\langle 2xy\rangle}{\langle x^2\rangle - \langle y^2\rangle}\right)\right] \tag{1}$$

where angle brackets denote ensemble average. A slight modification to consider the condition that the magnitude of $\langle y^2 \rangle$ exceeds $\langle x^2 \rangle$ is given by Hwang et al. (1997)

$$c = \tan\left\{\frac{1}{2}\left[\tan^{-1}\left(\frac{\langle 2xy\rangle}{\langle x^2\rangle - \langle y^2\rangle}\right) + \pi\right]\right\}, \quad \langle x^2\rangle < \langle y^2\rangle \tag{1b}$$

The regression coefficient based on minimizing the orthogonal distance differs from those obtained from minimizing the mean square distances in the y-direction, c_y, or in the x-direction, c_x:

$$c_y = \frac{\langle xy\rangle}{\langle x^2\rangle}, \tag{2}$$

and

$$c_x = \frac{\langle y^2\rangle}{\langle xy\rangle}, \tag{3}$$

When the correlation of the two data sets are high, these three coefficients become indistinguishable (see discussions in Bauer et al. 1992).

The average wave height and wind speed of the WAM output and TOPEX data are in good agreement from cycle to cycle. Figure 6 shows an example of the results. For the wave height, the rms difference for the 9-degree average is approximately 0.3 m, with a correlation coefficient of 0.93 for both tracks (Table 1). The rms difference increases to approximately 0.4 m when the averaging distance decreases and the correlation coefficient also decreases, possibly due to a decrease of data points in the averaging process. For the wind speed, the rms difference is 1.92 m/s for track 26 and 1.33 m/s for track 69, with the correlation coefficients of 0.83 and 0.91, respectively for the 9-degree average. The statistics for the 3-degree (Southern, Middle, and Northern) averages are also tabulated in Table 2. In general, the agreement in wave height between TOPEX and WAM are good, considering that the wind input used for driving the model is considerable difference from the TOPEX measurements.

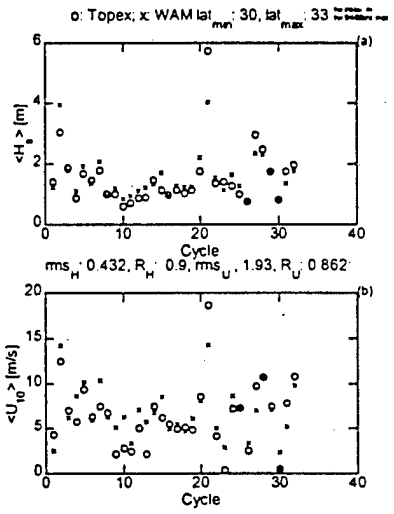

Figure 6. An example of the mean wave height (a) and wind speed (b) averaged along the track of various distances. The example shown is the 3-degree average (M3, from 30 to 33 degrees latitude). O: TOPEX, × = WAM. The statistics of comparison are listed in Table 1.

4. 2. Spatial Distribution

One of the most significant advantages of remote sensing measurements is the ability to provide a quasi-instantaneous measurement of the spatial distribution of the wave heights and wind speeds. For example, the 9° latitude transects of tracks 26 and 69 were completed in 168 and 190 s, respectively. The high spatial density of the measurements represents a unique source of wind and wave data that can be used for model comparison.

Figure 7 illustrates the cycle-by-cycle comparison of wave heights (top half) and wind speeds (bottom half) derived from WAM and TOPEX track 69. For this along-axis track, the WAM wave height output tends to be biased high in the first six to nine months of the year and the bias trend reverses toward the winter

months; however, the data scatter is quite large (Figure 8a). The bias trend of track 26 is slightly different, with the major negative bias appearing in the first four months, and positive the rest of the year. While there are apparent similarities of wave bias and wind bias, the scattering of data points is large. The average normalized bias relative to the mean wave height or wind speed, $B(H_S)/\langle H_S \rangle$, is 0.09 for track 26 and 0.08 for track 69. For wind speed ($B(U_{10})/\langle U_{10} \rangle$), the corresponding numbers are much larger, 0.39 and 0.57 for the two tracks.

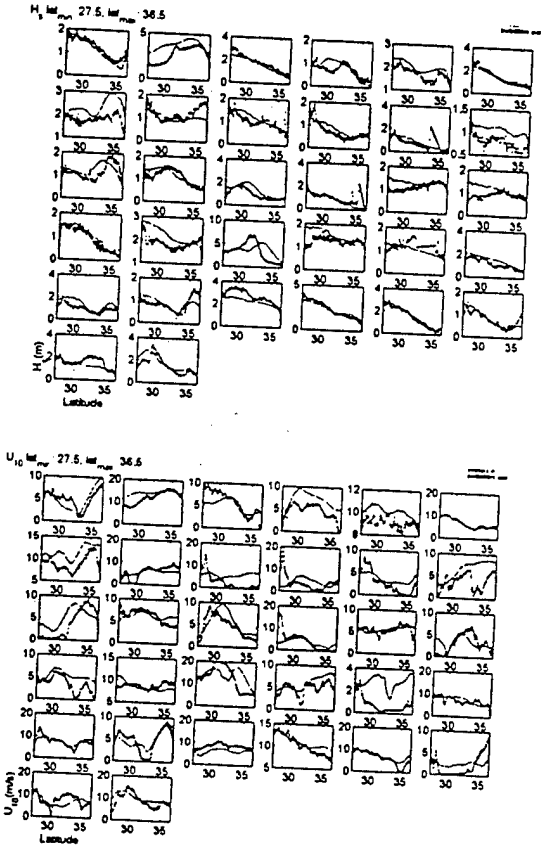

Figure 7. Track-by track comparison of the wave height (top half) and wind speed (bottom half) from TOPEX (dots) and WAM (solid curve).

The cycle-by-cycle normalized ($\Delta(H_S)/\langle H_S \rangle$, $\Delta(U_{10})/\langle U_{10} \rangle$) differences of wave heights and wind speeds are plotted in Figure 8c and 8d for tracks 26 and 69 respectively. The rms differences relative to the mean wave height are mostly less than 0.5, with an average value of 0.27 for track 26 and 0.24 for track 69. For wind speed, the corresponding numbers are 0.55 and 0.77 for the two tracks.

The linear regression coefficient, c, for tracks 26 and 69 is shown in Figures 8e and 8f. As can be seen from the plots, there are only small members of cases with $0.9 \le c \le 1.1$. The WAM output tends to over estimate the wave height, especially in the summer months. Many of the wave height over estimations can be associated with over estimation of the wind speed used as the input to the wave model. Exceptions are found in very low wind conditions, where the wave heights are mainly dominated by the swell components that are unrelated to the local wind condition.

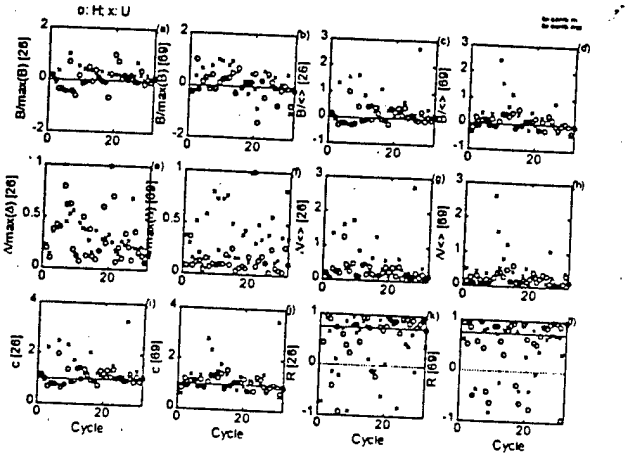

Figure 8. Statistics of comparing spatial distributions of WAM output with TOPEX measurements. Bias normalized by the maximum for track 26 (a) and 69 (b); bias normalized by the mean wave height or mean wind speed for track 26 (c) and 69 (d); rms difference normalized by the maximum for track 26 (e) and 69 (f); rms difference normalized by the mean wave height or mean wind speed for track 26 (g) and 69 (h); regression coefficient for track 26 (i) and 69 (j); and correlation coefficient for track 26 (k) and 69 (l). o: wave height, x: wind speed. (M3 averages).

The correlation coefficients between WAM and TOPEX data show the largest variation (Figure 8g and 8h) compared to the other statistical parameters. For the along-axis track 69, 7 out of 32 cycles show negative correlation coefficient, indicating that the opposite trends of wave height distribution along the altimeter track obtained from WAM modeling as compared to the altimeter measurements. In addition to the negative correlation cases, 9 more cycles have correlation coefficient of less than 0.75, so altogether one half of the cases examined for track 69 show poor correlation of WAM output with altimeter measurements. Similar to the wave correlation statistics, for the wind speed, there are 7 cycles of negative correlation and 9 additional cases of low correlation coefficients. While many cases of poor correlation in wind speeds correspond to those of poor correlation in wave heights, there are also many other mismatches.

Because the correlation coefficient is primarily a measure of proportionality of two variables (for example, when $y = cx^n$, where c and n are constant, the correlation coefficient always equals to unity) the correlation coefficient alone does not indicate the quantitative agreement of the two variables. The evaluation of data agreement needs to take into account other statistics such as the bias, rms difference and/or regression coefficient.

The cycle-by-cycle statistics of track 26 are not very different from those of track 69. For the wave height, there are 4 cases of negative correlation coefficient and 8 cases with $0 < R < 0.75$. For the wind speed, there are 9 negative correlation and 10 cases with $0 < R < 0.75$. Taking the statistics of the two tracks together, only in about one half of the cases are WAM output and TOPEX measurements in good agreement. The above conclusions are based on analyzing 32 cycles of 2 tracks over a 3-degree latitude stretch of the satellite tracks. Taking a different stretch, the statistics are not significantly different from the above results.

5. SUMMARY AND CONCLUSIONS

The wind speeds and wave heights measured by satellite altimeters have been compared with ocean buoy measurements with excellent agreement. They represent a good source of environmental data for the study of global and regional wave conditions. In this paper, we compare TOPEX altimeter measurements with WAM model output in the region of Yellow and East China Seas. Two of the satellite tracks passing through the region are selected for comparison. Track 69 passes through the central axis of YES and track 26 passes across the entrance to the enclosed seas. The comparisons are processed into two categories: (1) comparing the time series for a given location, and (2) comparing with the spatial distribution for a given time.

The first category is further divided into (a) average over a region from 3 to 9 degrees latitude along a track, and (b) seasonal average along a track. These average quantities from TOPEX and WAM are in good agreement in terms of mean and standard deviation of the statistics (Table 1). The difference between altimeter measurements and numerical simulations is approximately 10% with WAM overestimating most of the time. The median value of the rms differences is 0.4 m with a correlation coefficient of ~0.9 (Table 2). These figures are compared to 0.15 m and 0.97, respectively from TOPEX/buoy comparisons performed in the Gulf of Mexico region for comparable spatial and temporal separations (Hwang et al. 1997). The rms difference in wind speed in the YES/WAM comparison is ~2 m/s with a correlation coefficient of ~0.83. The corresponding values from TOPEX/buoy comparisons in the Gulf of Mexico region are 1.2 m/s and 0.9, respectively.

The comparison of spatial distributions of WAM simulations and TOPEX measurements is performed with 32 cycles each from the two tracks over 3 to 9 degrees latitude (Figure 7 shows the results of 9-degree processing). The quality of agreement between numerical simulations and altimeter measurements varies significantly from cycle to cycle. In many cases, opposite trends in the spatial distributions of wave heights and wind speeds are found. The statistics of bias, rms difference, linear regression coefficients and correlation coefficient from the 32 cycles of both tracks are analyzed (Figure 8 shows results of 3-degree averages). A rather large percentage (~50%) of cases show poor agreement based on a combination of low correlation and large rms difference or bias, and the regression coefficient differs significantly from one.

The comparisons presented here indicate that our numerical wave simulation skills are good in the projection of temporal evolution but relatively poor for the spatial variation of the wave field. The measurements from remote sensing devices, including spaceborne and airborne, are of spatial distribution in nature. These data represent a precious source for enhancing our understanding of the spatial properties of the wind and wave fields. The spaceborne data are especially useful for studying the regional wind and wave climate, in which case, the spatial density of in-situ measurements is usually not very high. Numerous comparison studies have shown that the accuracy of altimeter output of significant wave height and wind speed frequently exceeds the model output and is comparable in quality with in-situ ocean buoy measurements.

ACKNOWLEDGMENT

This research is sponsored by the Office of Naval Research (NRL Job Orders 6800-08, 7405-A8 and 6725-A8), and the U.S. Army Corps of Engineers. The WAM hindcast was conducted as part of the Military RDT&E Program of the U.S. Army Engineer Waterways Experiment Station's Coastal and Hydraulics Laboratory. Permission was granted by the Chief of Engineers to publish this information. [NRL contribution PP/7332—97-0025].

REFERENCES

Bauer, E., S. Hasselmann, and K. Hasselmann, , 1992: Validation and assimilation of Seasat altimeter wave heights using the WAM wave model, *J. Geophys. Res.*, 97, 12671-12682.

Bender, L. C., 1996: Modification of the physics and numerics in a third-generation ocean wave model.

J. Atmos. and Ocean. Tech., **13**, 726-750.

Bratos, S. M., 1997: Comparison between third generation and second generation ocean wave models. Masters Thesis, In review, Texas A&M University

Brown, G. S., H. R. Stanley, and N. A. Roy, 1981: The wind speed measurement capability of spaceborne radar altimeters, IEEE *J. Oceanic Eng.*, OE-6, 59-63.

Cardone, V. J. , 1992: On the structure of the marine surface wind field. 3rd International Workshop of Wave Hindcasting and Forecasting, Montreal, Quebec, May 19-22, 54-66.

Chelton, D. B., and F. J. Wentz, 1986: Further development of an improved altimeter wind speed algorithm, *J. Geophys. Res.*, 91, 14250-14260.

Ebuchi, N., and H. Kawamura, 1994: Validation of wind speeds and significant wave heights observed by the TOPEX altimeter around Japan, *J. Oceanography*, 50, 479--487.

Freilich, M. H., and P. G. Challenor, 1994: A new approach for determining fully empirical altimeter wind speed model functions, *J. Geophys. Res.*, 99, 25051-25062.

Gower, J.F.R., 1996: Intercomparison of wave and wind data from TOPEX/POSEIDON, *J. Geophys. Res.*, 101, 3817-3829.

Hwang, P. A., W. J. Teague, G. A. Jacobs, and D. N. Wang, 1997: A statistical comparison of wind speed, wave height and wave period derived from satellite altimeters and ocean buoys in the Gulf of Mexico region, subm. *J. Geophys, Res.*

Janssen, P. A. E. M., 1991: Quasi-linear theory of wind wave generation applied to wave forecasting. *J. Phys. Oceanogr.*, **21**, 745-754.

Lin, R. Q., and N. E. Huang, 1996: The Goddard Coastal Wave Model. Part I: Numerical method. *J. Phys. Oceanogr.*, **26**, 833-847.

Romeiser, R., 1993: Global validation of the wave model WAM over a one-year period using Geosat wave height data, *J. Geophys. Res.*, 98, 4713-4726.

Smith, W. H. F. and P. Wessel, 1990: Gridding with continuous curvature splines in tension, *Geophysics*, **55**, 293-305.

Tolman, H. L., 1992: Effects of numerics on the physics in a third-generation wind-wave model. *J. Phys. Oceanogr.*, **22**, 1095-1111.

WAMDI Group, 1988: The WAM model - a third generation wave prediction model. *J. Phys. Oceanogr.*, **18**, 1775-1810.

Wessel, P., and W. H. F. Smith, 1991: Free software helps map and display data. *EOS Trans. Amer. Geophys. U.*, **72**, 441, 445-446.

Wobus, R. L., and E. Kalnay, 1995: Three years of operational prediction of forecast skill at NMC. *Mon. Wea. Rev.*, **123**, 2132-2148.

Wang, Y., and D. G. Aubrey, 1987: The characteristics of China Coastline, *Cont. Shelf Res.*, 7, 329-349.

Witter, D. L., and D. B. Chelton, 1991: A Geosat altimeter wind speed algorithm and a method for altimeter wind speed algorithm development, *J. Geophys. Res.*, 96, 8853-8860.

Wu, J., 1992: Near-nadir microwave specular returns from the sea surface - altimeter algorithm for wind and wind stress, *J. Atm. Oceanic Tech.*, 9, 659-667.

Table 1. Comparison of Mean and Standard Deviation of WAM and TOPEX Average Data.

Latitude/Day limit	Wave Height				Wind Speed			
	$\langle H_s \rangle$ (m)		$\sigma_{Hs}/\langle H_s \rangle$		$\langle U_{10} \rangle$ (m/s)		$\sigma_{U10}/\langle U_{10} \rangle$	
	TOPEX	WAM	TOPEX	WAM	TOPEX	WAM	TOPEX	WAM
A. Annual average over a region								
(a) Track 26								
D9 (25.5, 34.5)	1.65	1.81	0.56	0.56	7.02	7.78	0.49	0.42
S3 (25.5, 28.5)	1.82	1.98	0.54	0.52	7.49	7.75	0.48	0.46
M3 (28.5, 31.5)	1.63	1.81	0.47	053	6.50	7.76	0.49	0.43
N3 (31.5, 34.5)	1.51	1.54	0.59	0.61	7.07	7.87	0.50	0.38
(b) Track 69								
D9 (27.5, 36.5)	1.45	1.55	0.58	0.54	6.66	6.94	0.51	0.49
S3 (27.5, 30.5)	1.70	1.85	0.45	0.37	7.19	6.99	0.46	0.51
M3 (30.5, 33.5)	1.49	1.53	0.65	0.55	6.66	6.97	0.52	0.45
N3 (33.5, 36.5)	1.16	1.21	0.58	0.74	6.15	6.84	0.53	0.50
B. Seasonal average along a track								
(a) Track 26								
Q1 (1, 90)	1.69	1.59	0.42	0.40	7.51	7.42	0.43	0.36
Q2 (91, 180)	1.10	1.31	0.28	0.31	4.78	6.50	0.47	0.35
Q3 181, 270)	1.84	2.14	0.69	0.72	7.06	7.21	0.64	0.63
Q4 (271, 360)	1.90	2.14	0.43	0.36	8.33	9.76	0.29	0.23
(b) Track 69								
Q1 (1, 90)	1.63	0.76	0.48	0.56	7.60	8.10	0.41	0.44
Q2 (91, 180)	0.96	1.07	0.40	0.36	4.50	5.17	0.57	0.38
Q3 (181, 270)	1.46	1.67	0.69	0.55	6.47	6.74	0.55	0.51
Q4 (271, 360)	1.69	1.67	0.50	0.50	7.85	7.76	0.38	0.45

Table 2. Statistical Coefficients of WAM and TOPEX Correlations.

	Wave Height, H_s					Wind Speed, U_{10}				
Latitude Limit	c_y	c	B (m)	Δ (m)	R	c_y	c	B (m/s)	Δ (m/s)	R
(a) Track 26										
D9 (25.5, 34.5)	1.06	1.07	0.13	0.33	0.93	1.10	1.13	1.07	1.92	0.83
S3 (25.5, 28.5)	1.07	1.09	0.17	0.43	0.92	1.02	1.04	0.37	1.73	0.87
M3 (28.5, 31.5)	1.07	1.09	0.15	0.41	0.91	1.16	1.21	1.60	2.56	0.78
N3 (31.5, 34.5)	1.03	1.06	0.06	0.41	0.90	1.09	1.13	1.20	2.52	0.75
(b) Track 69										
D9 (27.5, 36.5)	1.06	1.08	0.08	0.28	0.93	1.06	1.08	0.57	1.33	0.91
S3 (27.5, 30.5)	1.05	1.08	0.18	0.42	0.86	0.98	1.01	0.06	1.70	0.87
M3 (30.5, 33.5)	0.97	0.99	0.04	0.35	0.93	1.00	1.04	0.63	1.97	0.86
N3 (33.5, 36.5)	1.03	1.10	0.02	0.46	0.83	1.07	1.13	1.01	2.32	0.78